

[⁶Al] DISORDER IN AMPHIBOLES FROM MANTLE PERIDOTITES

ROBERTA OBERTI, FRANK C. HAWTHORNE*, LUCIANO UNGARETTI
AND ELIO CANNILLO

CNR Centro di Studio per la Cristallografia e la Cristallografia, via Abbiategrasso 209, I-27100 Pavia, Italy

ABSTRACT

The crystal structures of 15 amphiboles (pargasite and pargasitic hornblende) from the Finero mafic-ultramafic complex, Ivrea-Verbano Formation, Italy, have been refined to *R* indices of ~1.5% using MoK α X-ray data. Site populations were assigned from the results of site-scattering refinement and electron-microprobe analysis, combined with crystal-chemical analysis. Consideration of mean bond-lengths and chemical composition shows that these amphiboles have significant Al (up to 0.32 apfu) at the *M*(3) site, as well as considerable Al at the *M*(2) site. This is the first time that significant C-group Al has been observed at octahedrally coordinated sites other than *M*(2). There is no Al at the *M*(1) site; the amphibole structure seems to exert very stringent crystal-chemical constraints to prevent this particular occupancy, resulting from the inability of the structure to relax so as to accommodate the local bond-valence arrangement necessary for the occurrence of Al at the *M*(1) site. This finding of significant Al disorder over the *M*(2) and *M*(3) sites is in accord with infrared and ²H MAS NMR spectra of synthetic pargasite in the principal OH-stretching region. The results in the case of both natural and synthetic pargasite indicate that the main control on the degree of disorder is composition rather than conditions of crystallization. The significant (up to 11.5%) solid solution of a ferromagnesian amphibole component in the Finero amphiboles strongly correlates with the observed parageneses.

Keywords: amphibole, crystal-structure refinement, Al-disorder, peridotite, pargasite, Finero mafic-ultramafic complex, Ivrea-Verbano Zone, Italy.

SOMMAIRE

Nous avons affiné la structure cristalline de quinze échantillons d'amphibole, soit pargasite ou hornblende pargasitique, provenant du massif mafique-ultramafique de Finero, de la Formation de Ivrea-Verbano, en Italie, jusqu'à un résidu *R* d'environ 1.5% en utilisant des données de diffraction X (rayonnement MoK α). La population des sites a aussi été affinée, en tenant compte des concentrations documentées par microsonde électronique et des arguments cristallographiques. Une évaluation des longueurs moyennes des liaisons et de la composition chimique montre que cette suite contient une proportion importante d'aluminium dans le site *M*(3), jusqu'à 0.32 atomes par unité formulaire, ainsi qu'une proportion considérable dans le site *M*(2). C'est la première indication d'une proportion importante de l'aluminium de la position *C* à un site autre que *M*(2). Par contre, il n'y a pas d'aluminium dans le site *M*(1). La structure d'une amphibole semble exercer une contrainte cristallographique limitant très strictement une répartition impliquant *M*(1), ce qui l'empêche de se décontracter pour accommoder les agencements locaux des valences de liaison nécessaires autour de ce site. Notre découverte d'un désordre important impliquant *M*(2) et *M*(3) concorde avec les résultats de spectroscopie infrarouge et de résonance magnétique nucléaire de ²H par spin à l'angle magique, effectués sur la pargasite synthétique dans la région principale d'étirement de la liaison O-H. Les résultats obtenus sur la pargasite naturelle et synthétique montrent que la composition, plutôt que les conditions de formation, contrôlerait le degré de désordre. L'étendue de la solution solide envers une amphibole à Fe-Mg dans cette suite, jusqu'à 11.5%, montre une forte corrélation avec les paragenèses observées.

(Traduit par la Rédaction)

Mots-clés: amphibole, affinement de la structure cristalline, désordre, péridotite, pargasite, complexe mafique-ultramafique de Finero, zone de Ivrea-Verbano, Italie.

* Permanent address: Department of Geological Sciences, University of Manitoba, Winnipeg, Manitoba R3T 2N2.

INTRODUCTION

Amphibole of pargasitic or pargasitic hornblende composition can be an important liquidus phase in peridotites, and its crystallization can play an important role in the fractionation of peridotitic magmas (Cawthorn & O'Hara 1976). Most of our knowledge concerning the crystal chemistry of amphibole has been derived from the characterization of amphiboles formed at less extreme conditions (*i.e.*, lower temperatures and pressures, more common bulk-rock compositions); it is of both crystal-chemical and petrological interest to see if the behavior of amphiboles under extreme conditions is similar to that under more usual conditions. Under certain extreme conditions, amphiboles do show unusual characteristics of composition and order. For instance, richterite from lamproites can have significant $Ti^{4+} \rightarrow Si$ substitution, with Ti^{4+} completely ordered at the $T(2)$ site (Oberti *et al.* 1992); iron-rich alkali amphiboles from peralkaline granites can be an important sink for Li *via* the substitution $Li + Fe^{3+} \rightarrow 2 Fe^{2+}$, with Li completely ordered at the $M(3)$ site (Hawthorne *et al.* 1993). These examples involve extremes in bulk-rock composition. In the current work, we examine a sequence of rocks crystallized at high temperature and pressure to see if there are any unusual features in their constituent amphiboles.

The Finero mafic-ultramafic complex is part of the Ivrea-Verbano Formation, petrological and tectonic details of which are given by Rivalenti *et al.* (1975, 1981, 1984) and Ottonello *et al.* (1984). The Finero complex has been examined in detail by Cawthorn (1975), Coltorti & Siena (1984) and Siena & Coltorti (1989). It has four main units: (1) Phlogopite peridotite: dunite or harzburgite with amphibole and phlogopite, cut by rare amphibole-bearing dykes of chromitite, clinopyroxenite or websterite; (2) Layered internal zone (LIZ): amphibolite, metagabbro,

anorthosite, pyroxenite and peridotite; (3) Amphibole peridotite: amphibole-bearing peridotite, pyroxenite and amphibolite, and (4) External gabbro: gabbro with some pyroxenite – gabbro – anorthosite intercalations at the base.

All units contain amphibole, and the amphibole is never observed growing at the expense of clinopyroxene. Lensch (1968, 1976) has proposed that the widespread presence of amphibole and phlogopite in this suite is the result of crustal metasomatism. On the other hand, Cawthorn (1975), Coltorti & Siena (1984) and Siena & Coltorti (1989) have proposed that the amphibole is a primary liquidus phase: unit (1) is a slice of strongly depleted mantle tectonite, and the other three units are the associated layered complex. If one accepts the latter interpretation, the suite of Finero amphiboles are an ideal sequence to examine from a crystal-chemical viewpoint, as amphiboles are present in all units and show significant variations in chemical compositions as a function of paragenesis.

EXPERIMENTAL

The amphiboles used in this work, from the Finero mafic-ultramafic complex, were obtained from Franca Siena and Massimo Coltorti; petrological details are given by Coltorti & Siena (1984) and Siena & Coltorti (1989). Table 1 lists the original and current sample numbers, and the unit in which each amphibole occurs. Samples have been ordered according to the SE–NW sequence described by the above-mentioned authors.

X-ray data collection

Crystals were selected on the basis of optical clarity and freedom from inclusions, mounted on a Philips PW-1100 four-circle diffractometer, and examined with graphite-monochromated $MoK\alpha$ X-radiation; crystal quality was assessed *via* the profiles and widths

TABLE 1. SAMPLE IDENTIFICATION AND PROVENANCE OF AMPHIBOLES FROM FINERO

	Sample name	SEQ	Unit	Rock type	Paragenesis
F(1)	FE 122-2	290	Amphibole peridotite (SE)	pyroxenite	cpx+opx+amph+ol+op+sp1
F(2)	FE 280-2	282	Phlogopite peridotite	peridotite	ol+cpx+opx+sp1
F(3)	FE 134-1	281	Layered internal zone (SE)	peridotite	ol+amph+opx+sp1+op
F(4)	FE 81-1	286	External gabbro (SE)	amphibolite	amph+cpx+grt+op+ap
F(5)	FE 129-15	316	Layered internal zone (SE)	gabbro	p1+amph+grt+op+opx
F(6)	FE 121-2	288	Amphibole peridotite (SE)	amphibolite	amph+opx+cpx+ol+op+sp1
F(7)	FE 92-6	301	Amphibole peridotite (SE)	amphibolite	amph+ol+opx+cpx+sp1
F(8)	FE 92-1	284	Amphibole peridotite (SE)	amphibolite	amph+ol+opx+cpx+sp1
F(9)	FE 121-1	287	Amphibole peridotite (SE)	amphibolite	amph+opx+cpx+ol+op+sp1
F(10)	FE 228-1	300	Layered internal zone (NW)	olivine websterite	amph+opx+cpx+ol+sp1
F(11)	FE 229-10	315	Layered internal zone (NW)	sapphirine gabbro	p1+cpx+amph+spr+opx
F(12)	FE 229-1	297	Layered internal zone (NW)	sapphirine gabbro	p1+cpx+amph+spr+opx
F(13)	FE 214-1	298	Phlogopite peridotite	peridotite	ol+phl+amph+opx+op+cpx
F(14)	FE 229-14	318	Layered internal zone (NW)	sapphirine gabbro	p1+cpx+amph+spr+opx
F(15)	FE 229-18	328	Layered internal zone (NW)	sapphirine gabbro	p1+cpx+amph+spr+opx

SEQ = sequence number in Pavia amphibole data base

op = opaque minerals

of Bragg diffraction peaks. Unit-cell dimensions were calculated from least-squares refinement of the *d* values obtained from 35 rows of the reciprocal lattice by measuring the center of gravity of each reflection and of the corresponding antireflection in the θ range between -35 and $+35^\circ$. Intensity data were collected for two monoclinic equivalent pairs (*hkl* and $\bar{h}\bar{k}l$) in the θ range $2 < \theta < (55-60)^\circ$, depending on crystal size. Only the more intense reflections (those exceeding a predetermined counting threshold) were collected. For crystals F(5), F(11) and F(14), all reflections in the θ range $2-30^\circ$ were collected. Intensities were then corrected for absorption, Lorentz and polarization effects, averaged and reduced to structure factors. Only reflections with $I \geq 5\sigma(I)$ were considered as observed during the structure refinement.

Structure refinement

Structure refinement (SREF) procedures were as described by Oberti *et al.* (1992) following the model of Ungaretti (1980). In view of the short $\langle M(3)-O \rangle$ distances observed, the scattering curve for Al^{3+} was also used for the occupancy refinement of the *M*(3) site. Refinement information and final *R* indices are given in Table 2. Atomic positions and equivalent

isotropic displacement factors are given in Table 3, refined site-scattering values expressed as mean atomic numbers (MAN = scattering at $\sin \theta/\lambda = 0$) in Table 4, and selected interatomic distances and angles in Table 5. Structure factors and anisotropic displacement parameters may be obtained from the Depository of Unpublished Data, CISTI, National Research Council of Canada, Ottawa, Ontario K1A 0S2.

Electron-microprobe analysis

The crystals used in the collection of the crystallographic data were analyzed by electron microprobe according to the procedure of Oberti *et al.* (1992); average compositions are given in Table 6. Crystals F(2) and F(6) were lost during sample preparation and polishing. Unit formulae (Table 6) were recalculated on the basis of 24 (O,OH,F) apfu (atoms per formula unit) and using the Fe^{3+}/Fe^{2+} values derived from the structure refinement. The structure refinements show no significant oxy-component in these amphiboles [based on *M*(1)–*M*(1) and *M*(1)–O(3) distances], and thus O(3) is occupied by (OH + F).

SITE POPULATIONS:
QUALITATIVE CONSIDERATIONS

The site populations in this suite of amphiboles are of particular interest, as it has been suggested (Siena & Coltorti 1989) that these amphiboles are an early liquidus phase rather than a product of metamorphic reaction. The unusual nature of the site populations in these amphiboles is indicated by the extremely short $\langle M(3)-O \rangle$ distances (Table 5), which range from 2.045 to 2.071 Å. The $\langle M(3)-O \rangle$ distance in amphibole is significantly shortened by F substitution at the O(3) site, ~ 0.013 Å per F atom per formula unit (apfu); however, in the present case, electron-microprobe analysis (Table 6) indicates negligible (<0.10 apfu) F at O(3). This means that the *M*(3) site must be occupied by significant amounts of cations smaller than Mg. This behavior is best shown by the relationship between the $\langle M(3)-O \rangle$ distance and the observed MAN (Mean Atomic Number) at the *M*(3) site (Fig. 1a). Also shown in Figure 1a is the range observed in ~ 350 calcic amphiboles with negligible monovalent-anion deficiency at O(3) (taken from the Pavia amphibole database). For these latter amphiboles, *M*(3) is occupied mainly by Mg and Fe^{2+} , and O(3) is occupied mainly by (OH). The Finero amphiboles (solid circles) fall well outside this field, the departures being in the range 0.004–0.022 Å. There is a tendency toward increasing $\langle M(3)-O \rangle$ with increasing $M^{(3)}$ MAN, but more notable is the variation of 0.021 Å in $\langle M(3)-O \rangle$ for almost constant $M^{(3)}$ MAN values close to 13.6 *e* (Tables 4, 5).

The *M*(1) site does not show this type of behavior (Fig. 1b). The Finero amphiboles lie at the upper limit

TABLE 2. UNIT-CELL DIMENSIONS, REFLECTION INFORMATION AND *R* INDICES FOR THE AMPHIBOLES FROM FINERO

	F(1)	F(2)	F(3)	F(4)	F(5)	F(6)	F(7)	F(8)
<i>a</i> (Å)	9.873	9.890	9.867	9.860	9.828	9.869	9.866	9.861
<i>b</i>	18.011	18.024	17.998	17.984	17.917	17.990	17.994	17.959
<i>c</i>	5.299	5.292	5.285	5.290	5.290	5.293	5.291	5.289
β ($^\circ$)	105.17	105.25	105.19	105.26	105.16	105.30	105.24	105.32
<i>V</i> (Å ³)	909.5	910.1	905.7	905.0	899.2	906.5	906.2	903.3
θ_{max} ($^\circ$)	55	55	55	55	30	55	60	55
# <i>F</i> _{h11}	1781	1179	1285	1517	1371	1312	1079	1268
# <i>F</i> _{obs}	1761	1177	1281	1514	1088	1307	1075	1258
<i>R</i> _{sym} %	1.90	1.46	1.50	1.30	0.80	2.00	1.20	2.30
<i>R</i> _{obs} %	1.53	1.25	1.20	1.11	1.34	1.33	1.28	2.56
<i>R</i> _{h11} %	1.55	1.25	1.20	1.11	2.20	1.34	1.29	2.56
	F(9)	F(10)	F(11)	F(12)	F(13)	F(14)	F(15)	
<i>a</i> (Å)	9.874	9.871	9.857	9.854	9.886	9.855	9.854	
<i>b</i>	17.995	17.962	17.932	17.935	18.009	17.927	17.931	
<i>c</i>	5.298	5.279	5.285	5.285	5.291	5.283	5.282	
β ($^\circ$)	105.40	105.22	105.36	105.31	105.24	105.44	105.33	
<i>V</i> (Å ³)	907.5	903.1	900.9	900.8	908.9	899.7	900.2	
θ_{max} ($^\circ$)	55	60	30	60	60	30	60	
# <i>F</i> _{h11}	1483	2237	1365	2496	1266	1358	3004	
# <i>F</i> _{obs}	1480	2187	1062	2466	1261	1024	2962	
<i>R</i> _{sym} %	1.40	1.60	1.20	1.30	1.30	1.40	1.20	
<i>R</i> _{obs} %	1.53	1.56	1.23	1.59	1.16	1.36	1.60	
<i>R</i> _{h11} %	1.53	1.56	1.23	1.59	1.17	1.36	1.63	

Note: e.s.d.s are ≤ 0.002 for *a* and *c*, ≤ 0.004 for *b*, $\leq 0.01^\circ$ for β . The space group is *C2/m*.

TABLE 3. ATOMIC COORDINATES ($\times 10^4$) AND EQUIVALENT ISOTROPIC DISPLACEMENT FACTORS (\AA^2) FOR THE AMPHIBOLES FROM FINERO

	F(1)	F(2)	F(3)	F(4)	F(5)	F(6)	F(7)	F(8)	F(9)	F(10)	F(11)	F(12)	F(13)	F(14)	F(15)	
O(1)	x	1070	1077	1065	1073	1060	1065	1071	1068	1068	1067	1059	1060	1078	1059	1062
	y	861	870	883	875	886	878	874	873	879	871	875	875	872	874	873
	z	2154	2173 ^a	2152	2162	2140	2154	2159	2156	2156	2156	2142	2146	2173	2145	2148
O(2)	B	0.78	0.71	0.79	0.77	0.82	0.83	0.79	0.89	0.81	0.83	0.92	0.90	0.65	0.91	0.89
	x	1196	1197	1199	1195	1198	1197	1194	1196	1198	1198	1197	1196	1194	1197	1197
	y	1738	1728	1741	1732	1741	1737	1732	1734	1737	1735	1736	1736	1728	1736	1736
O(3)	z	7327	7301	7341	7321	7356	7334	7324	7324	7331	7328	7347	7346	7303	7345	7344
	B	0.63	0.61	0.67	0.64	0.64	0.68	0.66	0.74	0.65	0.64	0.69	0.66	0.58	0.68	0.67
	x	1085	1080	1086	1084	1085	1081	1081	1082	1085	1077	1074	1076	1084	1073	1074
O(4)	B	0.80	0.75	0.84	0.77	0.76	0.83	0.80	0.86	0.79	0.79	0.85	0.83	0.68	0.86	0.82
	x	3680	3663	3682	3671	3688	3677	3673	3670	3674	3673	3679	3677	3665	3680	3677
	y	2498	2494	2501	2500	2504	2501	2499	2500	2500	2501	2505	2505	2494	2505	2505
O(5)	z	7882	7881	7882	7884	7878	7877	7876	7870	7880	7868	7871	7875	7891	7868	7870
	B	0.86	0.81	0.88	0.85	0.91	0.86	0.85	0.95	0.83	0.86	0.92	0.88	0.79	0.94	0.88
	x	3499	3486	3503	3496	3506	3501	3496	3495	3500	3504	3507	3507	3484	3507	3507
O(6)	y	1404	1394	1408	1403	1412	1410	1405	1407	1407	1414	1416	1417	1389	1419	1419
	z	1122	1107	1130	1121	1134	1131	1126	1136	1135	1141	1146	1151	1102	1153	1153
	B	0.86	0.89	0.86	0.86	0.83	0.87	0.89	0.96	0.86	0.85	0.88	0.86	0.84	0.86	0.86
O(7)	x	3435	3439	3436	3437	3432	3434	3435	3437	3437	3436	3433	3434	3436	3431	3434
	y	1162	1160	1162	1163	1161	1160	1160	1160	1162	1151	1152	1153	1165	1151	1150
	z	6094	6083	6109	6090	6109	6115	6098	6112	6112	6136	6146	6143	6062	6149	6148
O(7)	B	0.97	0.96	0.99	0.96	1.00	1.01	0.98	1.09	0.98	0.99	1.05	1.02	0.88	1.04	1.02
	x	3395	3395	3400	3394	3393	3398	3400	3398	3398	3411	3410	3410	3385	3412	3412
	y	2744	2769	2731	2753	2720	2725	2739	2730	2731	2696	2694	2685	2692	2686	2686
T(1)	B	1.08	1.16	1.07	1.11	1.08	1.10	1.13	1.22	1.11	1.00	1.09	1.04	1.09	1.05	1.04
	x	2806	2801	2805	2807	2807	2807	2807	2807	2806	2807	2807	2807	2798	2808	2808
	y	853	850	854	852	855	853	852	852	853	852	854	854	851	854	854
T(2)	z	3022	3022	3024	3022	3023	3028	3023	3023	3026	3028	3031	3030	3020	3033	3031
	B	0.38	0.42	0.42	0.42	0.35	0.41	0.42	0.52	0.43	0.40	0.46	0.43	0.38	0.46	0.43
	x	2909	2900	2911	2905	2915	2909	2907	2908	2907	2908	2910	2910	2898	2910	2911
M(1)	y	1728	1726	1731	1729	1733	1731	1729	1730	1730	1731	1734	1734	1726	1734	1734
	z	8124	8111	8134	8122	8136	8131	8123	8127	8130	8130	8139	8139	8110	8141	8139
	B	0.44	0.46	0.46	0.46	0.43	0.47	0.46	0.55	0.46	0.44	0.50	0.45	0.41	0.49	0.46
M(2)	x	892	887	894	889	895	892	889	890	892	893	894	894	888	894	894
	y	0.50	0.52	0.49	0.50	0.47	0.51	0.51	0.63	0.52	0.48	0.53	0.50	0.45	0.51	0.50
	z	1768	1762	1764	1762	1765	1764	1761	1762	1763	1762	1762	1762	1762	1761	1762
M(3)	B	0.47	0.52	0.47	0.47	0.45	0.52	0.48	0.57	0.48	0.46	0.54	0.47	0.44	0.50	0.47
	x	0.49	0.52	0.47	0.46	0.46	0.49	0.46	0.55	0.48	0.45	0.50	0.48	0.44	0.48	0.46
	y	2799	2794	2801	2798	2794	2798	2796	2799	2800	2800	2796	2800	2795	2796	2801
M(4)	z	0.67	0.75	0.69	0.67	0.74	0.72	0.71	0.78	0.70	0.61	0.77	0.62	0.67	0.73	0.61
	B	2586	2557	2585	2571	2527	2548	2545	2534	2554	2587	2543	2586	2559	2544	2592
	x	0.50	0.80	0.66	0.69	0.49	0.46	0.57	0.73	0.67	0.94	0.87	0.80	0.59	0.89	0.79
A	B	5.28	2.66	4.92	4.91	5.12	5.76	3.13	3.64	5.26	5.14	2.36	5.72	1.05	1.86	6.39
	x	359	319	336	291	200	268	220	139	292	257	254	169	286	264	232
	y	904	802	843	727	611	752	766	586	748	768	801	583	657	833	501
A(2)	B	3.97	2.85	5.33	4.80	3.12	5.09	2.55	3.22	3.65	3.23	5.31	3.78	3.39	2.93	5.80
	x	4682	4685	4675	4675	4690	4680	4694	4664	4673	4694	4683	4696	4682	4678	4691
	y	1.40	1.90	1.79	1.66	1.61	1.33	2.11	1.74	1.33	1.91	1.26	1.82	2.38	1.25	1.32
H	z	1908	1921	1850	1974	1902	1857	1973	2030	1897	1853	1955	1926	1976	1835	1893
	B	7618	7548	7650	7676	7667	7477	7625	7277	7583	7606	7555	7648	7615	7725	7677
	x	1.18	4.39	2.00	4.31	1.46	3.41	2.22	6.24	0.58	0.79	2.69	2.27	2.65	2.05	1.67

Note: O(3) = x,0,z; O(7) = x,0,z; M(1) = 0,y,1/2; M(2) = 0,y,0; M(3) = 0,0,0; M(4) = 0,y,1/2; M(4') = 0,y,1/2; A = 0,1/2,0; A(m) = x,1/2,z; A(2) = 0,y,0; H = x,0,z.

TABLE 4. REFINED SITE-SCATTERING VALUES (EPFU) IN AMPHIBOLES FROM FINERO

M*	F(1)	F(2)	F(3)	F(4)	F(5)	F(6)	F(7)	F(8)	
M(1)	2	30.24	26.60	28.76	26.55	27.75	28.45	26.32	26.66
M(2)	2	30.70	28.57	30.29	28.69	27.86	29.95	28.71	28.90
M(3)	1	15.78	13.79	15.14	13.67	14.55	14.84	13.53	13.62
M(4)	2	41.00	40.54	40.73	40.59	40.95	40.90	40.69	41.08
A	1	9.02	9.43	9.39	8.25	8.54	9.54	8.33	8.72
M*	F(9)	F(10)	F(11)	F(12)	F(13)	F(14)	F(15)		
M(1)	2	28.37	26.66	26.16	26.18	26.18	26.10	26.13	
M(2)	2	30.24	27.70	26.54	26.34	28.38	26.38	26.26	
M(3)	1	14.77	13.77	13.61	13.60	13.48	13.51	13.48	
M(4)	2	40.85	40.66	40.37	40.01	40.42	40.22	39.89	
A	1	9.12	9.98	10.15	9.98	8.95	10.05	10.23	

M* = multiplicity of site in the structural formula.

of $\langle M(1)-O \rangle$ for a given $M^{(1)}MAN$ in calcic amphiboles, indicating that no trivalent cation is present at $M(1)$. Thus the $M(1)$ site is occupied by Mg and Fe^{2+} , whereas the $M(3)$ site must be occupied by (at least) one cation significantly smaller than either Mg or Fe^{2+} . We note that $[6]R^{3+}$ occurs at the $M(1)$ site only where associated with dehydrogenation at the adjacent O(3) site; there is no evidence of dehydrogenation [*i.e.*, a divalent anion at O(3)] in these Finero amphiboles.

The distribution of $\langle M(1)-O \rangle$ and $\langle M(3)-O \rangle$ distances is also a good indicator of this unusual behavior. In general, the $M(1)$ and $M(3)$ sites are occupied by Mg and Fe^{2+} (Ungaretti 1980, Hawthorne 1983), and the distribution of Mg and Fe^{2+} between $M(1)$ and $M(3)$ is usually very regular (*e.g.*, Ungaretti *et al.* 1981), K_d varying between ~ 1.0 for $M(2)$ occupied by (Mg, Fe^{2+}) and 0.40 for $M(2)$ occupied by (Al, Fe^{3+}). As

TABLE 5. SELECTED INTERATOMIC DISTANCES (Å) IN AMPHIBOLES FROM FINERO

	F(1)	F(2)	F(3)	F(4)	F(5)	F(6)	F(7)	F(8)	F(9)	F(10)	F(11)	F(12)	F(13)	F(14)	F(15)
T(1)-O(1)	1.655	1.646	1.658	1.650	1.659	1.658	1.654	1.655	1.655	1.658	1.662	1.661	1.641	1.662	1.660
T(1)-O(5)	1.682	1.676	1.683	1.678	1.680	1.686	1.680	1.677	1.683	1.686	1.688	1.687	1.671	1.689	1.687
T(1)-O(6)	1.678	1.672	1.680	1.674	1.679	1.681	1.676	1.680	1.682	1.682	1.685	1.685	1.666	1.683	1.684
T(1)-O(7)	1.662	1.659	1.666	1.657	1.659	1.665	1.661	1.659	1.664	1.668	1.669	1.669	1.652	1.669	1.670
<T(1)-O>	1.669	1.663	1.672	1.665	1.669	1.672	1.668	1.668	1.671	1.674	1.676	1.675	1.657	1.676	1.675
T(2)-O(2)	1.633	1.625	1.631	1.627	1.629	1.630	1.630	1.628	1.627	1.629	1.629	1.629	1.626	1.628	1.629
T(2)-O(4)	1.603	1.597	1.602	1.599	1.601	1.602	1.600	1.598	1.601	1.598	1.600	1.600	1.596	1.602	1.600
T(2)-O(5)	1.649	1.650	1.643	1.647	1.644	1.645	1.648	1.648	1.649	1.645	1.644	1.645	1.651	1.643	1.644
T(2)-O(6)	1.662	1.666	1.658	1.663	1.656	1.660	1.662	1.658	1.662	1.659	1.659	1.659	1.667	1.659	1.659
<T(2)-O>	1.637	1.635	1.634	1.634	1.632	1.634	1.635	1.633	1.635	1.633	1.633	1.633	1.635	1.633	1.633
M(1)-O(1) x2	2.056	2.052	2.049	2.052	2.049	2.052	2.052	2.051	2.055	2.048	2.051	2.050	2.053	2.050	2.049
M(1)-O(2) x2	2.116	2.103	2.118	2.106	2.115	2.113	2.107	2.105	2.112	2.106	2.105	2.105	2.101	2.104	2.104
M(1)-O(3) x2	2.097	2.090	2.099	2.092	2.092	2.096	2.093	2.091	2.096	2.095	2.092	2.094	2.090	2.091	2.094
<M(1)-O>	2.089	2.082	2.088	2.083	2.085	2.087	2.084	2.083	2.088	2.083	2.083	2.083	2.081	2.082	2.083
M(2)-O(1) x2	2.083	2.097	2.070	2.082	2.056	2.076	2.083	2.080	2.076	2.082	2.068	2.069	2.094	2.067	2.073
M(2)-O(2) x2	2.068	2.082	2.060	2.069	2.051	2.057	2.067	2.068	2.071	2.065	2.056	2.057	2.078	2.060	2.058
M(2)-O(4) x2	1.985	2.006	1.983	1.990	1.971	1.986	1.994	1.991	1.988	1.991	1.979	1.979	2.002	1.977	1.980
<M(2)-O>	2.045	2.062	2.038	2.047	2.026	2.043	2.048	2.046	2.045	2.046	2.035	2.035	2.058	2.035	2.037
M(3)-O(1) x4	2.075	2.066	2.073	2.065	2.067	2.066	2.063	2.057	2.068	2.055	2.052	2.052	2.069	2.050	2.050
M(3)-O(3) x2	2.063	2.057	2.058	2.055	2.055	2.053	2.049	2.050	2.060	2.040	2.042	2.040	2.060	2.040	2.036
<M(3)-O>	2.071	2.063	2.068	2.062	2.063	2.062	2.058	2.054	2.065	2.050	2.049	2.048	2.066	2.046	2.045
M(4)-O(2) x2	2.409	2.412	2.409	2.410	2.394	2.407	2.409	2.407	2.409	2.410	2.402	2.409	2.411	2.399	2.408
M(4)-O(4) x2	2.315	2.325	2.312	2.320	2.301	2.316	2.315	2.316	2.323	2.311	2.310	2.314	2.327	2.308	2.311
M(4)-O(5) x2	2.624	2.647	2.610	2.621	2.607	2.610	2.621	2.609	2.610	2.597	2.593	2.587	2.652	2.586	2.583
M(4)-O(6) x2	2.587	2.595	2.585	2.582	2.588	2.595	2.592	2.589	2.590	2.604	2.609	2.601	2.584	2.613	2.604
<M(4)-O>	2.484	2.495	2.479	2.483	2.472	2.482	2.484	2.480	2.483	2.480	2.479	2.477	2.493	2.477	2.477
<A-O>	2.934	2.933	2.930	2.932	2.923	2.930	2.930	2.926	2.931	2.917	2.915	2.917	2.939	2.915	2.914
<A(m)-O>	2.896	2.900	2.897	2.906	2.914	2.907	2.906	2.923	2.907	2.897	2.894	2.916	2.914	2.892	2.919
<A(2)-O>	2.600	2.604	2.589	2.594	2.594	2.593	2.603	2.581	2.590	2.588	2.579	2.589	2.610	2.576	2.583

<M(1)-O> and <M(3)-O> are linear functions of the sizes of the constituent cations (Hawthorne 1978, Cannillo *et al.* 1981), usually there will be a linear relationship between <M(1)-O> and <M(3)-O> (particularly *within* each of the calcic, sodic-calcic and alkali amphibole groups). This is shown in Figure 2 for the (F,OH)-bearing calcic amphiboles. The Finero amphiboles (solid circles) depart significantly from this trend. It is noteworthy that all pargasite structures in the Pavia amphibole database show <M(1)-O> and <M(3)-O> distances respectively longer and shorter than those observed for other calcic amphiboles

(dashed area in Fig. 2). This may be due partly to structural relaxation resulting from local charge-balance constraints (as we shall discuss later); however, the very short <M(3)-O> distances in the Finero crystals do imply the presence of trivalent cations at M(3).

So what cations occupy the M(3) site? From the observed site-scattering values, the principal cations must have an atomic number $Z \approx 13$, *i.e.*, Mg and Al; the smaller amounts of stronger scatterers can only be Fe²⁺ and Fe³⁺. Both of these conclusions are in accord with the observed unit formulae (Table 6). Thus M(3)

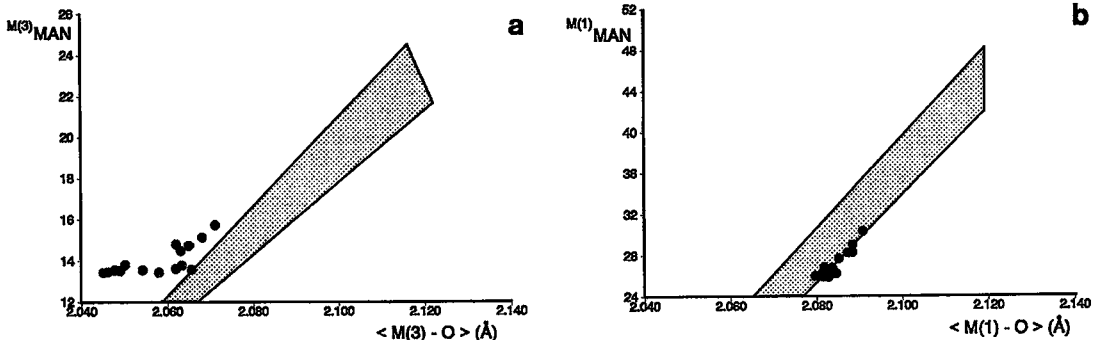


FIG. 1. Variation in the scattering (MAN) at the M(1) and M(3) sites as a function of the <M-O> distance for the Finero suite of amphibole compositions (solid circles); also shown is the range of variation for calcic hydroxy-amphiboles observed in the Pavia amphibole database: (a) M(3) site; (b) M(1) site.

TABLE 6. CHEMICAL COMPOSITION OF CRYSTALS USED IN THE STRUCTURE REFINEMENT

	F(1)	F(3)	F(4)	F(5)	F(7)	F(8)	F(9)	F(10)	F(11)	F(12)	F(13)	F(14)	F(15)
SiO ₂	42.71	42.37	46.61	43.14	44.53	43.92	42.93	43.08	42.64	42.88	46.44	42.44	42.99
Al ₂ O ₃	13.50	14.53	12.97	15.74	13.23	13.64	14.28	15.28	16.73	16.76	10.08	16.85	16.96
TiO ₂	1.23	0.28	0.45	0.14	0.33	0.35	0.48	0.23	0.08	0.11	0.59	0.10	0.12
Cr ₂ O ₃	0.59	0.09	0.24	0.01	0.53	0.40	0.42	0.23	0.39	0.28	1.90	0.15	0.28
*Fe ₂ O ₃	0.45	2.04	0.66	1.11	1.11	1.29	0.83	0.46	0.19	0.09	0.28	0.09	0.19
FeO	8.36	6.80	4.83	5.76	3.88	3.98	6.58	4.59	3.46	3.54	2.91	3.70	3.46
MnO	0.12	0.11	0.08	0.05	0.09	0.08	0.10	0.05	0.05	0.06	0.05	0.06	0.05
NiO	0.04	0.05	0.00	0.01	0.07	0.09	0.06	0.09	0.12	0.12	0.11	0.11	0.10
MgO	15.20	15.65	17.29	16.49	18.10	17.82	16.23	17.62	17.77	17.88	19.39	17.71	17.81
CaO	11.90	12.01	12.45	11.44	12.20	12.16	12.06	11.91	11.70	11.78	12.57	11.82	11.66
Na ₂ O	2.63	2.74	2.18	2.73	2.45	2.52	2.76	3.21	3.45	3.34	1.93	3.37	3.41
K ₂ O	0.21	0.03	0.19	0.13	0.20	0.22	0.16	0.05	0.07	0.06	0.94	0.04	0.06
F	0.02	0.02	0.00	0.05	0.01	0.04	0.06	0.04	0.13	0.06	0.18	0.06	0.07
Cl	0.07	0.11	0.00	0.06	0.01	0.01	0.02	0.07	0.02	0.01	0.01	0.02	0.02
H ₂ O	(2.03)	(2.01)	(2.12)	(2.04)	(2.08)	(2.06)	(2.03)	(2.05)	(2.04)	(2.08)	(2.02)	(2.06)	(2.07)
O=F,Cl	-0.03	-0.04	0.00	-0.04	-0.01	-0.02	-0.03	-0.04	-0.07	-0.03	-0.08	-0.03	-0.03
Total	99.03	98.80	100.07	98.86	98.81	98.56	98.97	98.92	98.77	99.02	99.32	98.55	99.22
Chemical formulae:													
Si	6.234	6.170	6.565	6.201	6.372	6.312	6.218	6.176	6.086	6.100	6.610	6.074	6.100
Al	1.766	1.830	1.435	1.799	1.628	1.688	1.782	1.824	1.914	1.900	1.390	1.926	1.900
Sum T	8.000	8.000	8.000	8.000	8.000	8.000	8.000	8.000	8.000	8.000	8.000	8.000	8.000
Al	0.557	0.664	0.718	0.868	0.603	0.622	0.656	0.758	0.901	0.910	0.301	0.917	0.937
Ti	0.135	0.031	0.048	0.015	0.036	0.038	0.052	0.025	0.009	0.012	0.063	0.011	0.013
Cr ³⁺	0.068	0.010	0.027	0.001	0.060	0.046	0.048	0.026	0.044	0.032	0.214	0.017	0.031
Fe ²⁺	0.049	0.224	0.070	0.120	0.120	0.140	0.090	0.050	0.020	0.010	0.030	0.010	0.020
Fe ³⁺	1.020	0.828	0.569	0.692	0.464	0.478	0.798	0.550	0.413	0.421	0.346	0.443	0.411
Mn ²⁺	0.015	0.014	0.009	0.006	0.011	0.010	0.012	0.006	0.006	0.007	0.006	0.007	0.006
Mg	3.308	3.396	3.631	3.534	3.862	3.818	3.503	3.767	3.782	3.793	4.115	3.780	3.768
Ni	0.005	0.005	n.d.	0.001	0.008	0.010	0.007	0.010	0.014	0.014	0.013	0.013	0.011
Sum C	5.157	5.172	5.072	5.237	5.164	5.162	5.166	5.192	5.189	5.199	5.088	5.198	5.197
A	0.157	0.172	0.072	0.237	0.164	0.162	0.166	0.192	0.189	0.199	0.088	0.198	0.197
Ca	1.861	1.880	1.879	1.762	1.870	1.872	1.868	1.830	1.789	1.796	1.917	1.813	1.773
Na	-	-	0.049	0.001	-	-	-	-	0.022	0.005	-	-	0.030
Sum B	2.018	2.052	2.000	2.000	2.034	2.034	2.034	2.022	2.000	2.000	2.005	2.011	2.000
Na	0.744	0.774	0.546	0.760	0.680	0.702	0.775	0.892	0.933	0.916	0.533	0.935	0.908
K	0.039	0.006	0.034	0.024	0.037	0.040	0.030	0.009	0.013	0.011	0.171	0.007	0.011
Sum A	0.783	0.780	0.580	0.784	0.717	0.742	0.805	0.901	0.946	0.927	0.704	0.942	0.919
F	0.009	0.009	n.d.	0.023	0.005	0.018	0.028	0.018	0.059	0.027	0.081	0.027	0.031
Cl	0.017	0.027	n.d.	0.015	0.002	0.002	0.005	0.017	0.005	0.002	0.002	0.005	0.005
OH	(1.974)	(1.964)	(2.000)	(1.982)	(1.993)	(1.980)	(1.967)	(1.965)	(1.936)	(1.971)	(1.917)	(1.968)	(1.964)

* derived from SREF (see text)

can be occupied by Mg, Fe²⁺, Al and Fe³⁺; moreover, as indicated in Figure 1a, M(3) must contain significant amounts of cations smaller than Mg, namely Al or Fe³⁺. There are three factors suggesting that only Al is of importance in this regard in the Finero amphiboles: (1) the amounts of Fe³⁺ derived from the structure refinement results are very small, and could not possibly have an effect of the magnitude shown in Figure 1a; (2) as we shall see later, the departure from

ideality in Figure 1a is *inversely* correlated with the amount of Fe present in the crystal, and it is notable that the crystal with the largest departure from the expected value [F(15), in which the departure is 0.022 Å] has the lowest Fe content of all these compositions; (3) the observed scattering at the M(3) site shows the Fe content at this site to be insufficient to cause the observed <M(3)-O> bond distances. Thus Al *must* be the principal small cation at the M(3) site.

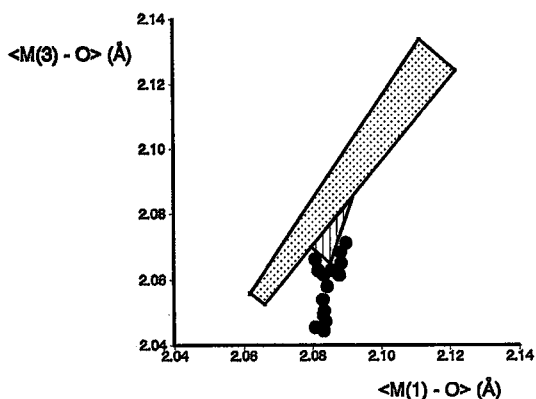


FIG. 2. Variation in $\langle M(1)-O \rangle$ and $\langle M(3)-O \rangle$; same symbols as in Fig. 1. The dashed area represents the field of the other pargasite crystals in the Pavia database.

SITE POPULATIONS:
QUANTITATIVE ASSIGNMENTS

Comparison of X-ray and electron-microprobe results

Site-scattering refinement (SREF) and electron-microprobe analysis (EMPA) plus unit-formula calculation provide independent estimates of the scattering power at the (A + B + C) sites; the average agreement between these two estimates is 0.36 electrons (0.3% relative). The only significant disagreement (SREF – EMPA = -1.52 e) is for sample F(4); without F(4), the

agreement is 0.26 e (0.2%). Thus the agreement between the two sets of results is very good, and it is possible to obtain reliable site-populations simply by partitioning the cation content obtained by EMPA with the help of the information (MAN and $\langle M-O \rangle$) obtained from SREF. This will be done in the following sections.

A site

The various A-sites are occupied predominantly by Na and vacancy, with only small amounts of K present. The average |SREF – EMPA| disagreement is 0.23 e for all the crystals but F(4), for which it is 1.6 e.

M(4) site

Both the site-scattering results and the unit formulae from electron-microprobe analysis show M(4) to be occupied by Ca and a small amount of C-group cations. The fact that the refined site-scattering at M(4) usually exceeds 40 electrons per formula unit (epfu) indicates that (Fe²⁺, Mn²⁺) are the dominant C-group cations at the M(4') site, the split position with [6+2] coordination that hosts the small M(4) cations in amphiboles [see Oberti *et al.* (1993) for more details]. M(4') always shows significant occupancy in these amphiboles, and Mn²⁺ was assigned to the M(4') site in view of its very strong preference for M(4') in ferromagnesian amphiboles. The (Mn²⁺ + Fe²⁺ + Mg) contents of M(4') were assigned such as to bring the B- and C-group cations into optimum agreement with the refined scattering values at the M(4) and M(1,2,3) sites, respectively. The resulting site-populations are reported in Table 7.

TABLE 7. M-SITE POPULATIONS IN FINERO AMPHIBOLES

		F(1)	F(3)	F(4)	F(5)	F(7)	F(8)	F(9)	F(10)	F(11)	F(12)	F(13)	F(14)	F(15)
M(1)	Mg	1.57	1.68	1.82	1.74	1.84	1.83	1.72	1.82	1.86	1.84	1.85	1.85	1.85
	*Fe ²⁺	0.43	0.32	0.18	0.26	0.16	0.17	0.28	0.18	0.14	0.16	0.15	0.15	0.15
M(2)	Ti	0.13	0.03	0.05	0.01	0.04	0.04	0.05	0.03	0.01	0.01	0.06	0.01	0.01
	Cr	0.07	0.01	0.03	0.00	0.06	0.04	0.05	0.03	0.04	0.03	0.21	0.02	0.03
	Al	0.44	0.53	0.46	0.72	0.40	0.42	0.49	0.48	0.62	0.64	0.20	0.65	0.60
	Fe ³⁺	0.05	0.22	0.07	0.12	0.12	0.14	0.09	0.05	0.02	0.01	0.03	0.01	0.02
	*Fe ²⁺	0.23	0.16	0.17	0.09	0.09	0.09	0.22	0.13	0.07	0.08	0.02	0.10	0.07
	Mg	1.08	1.05	1.22	1.06	1.29	1.27	1.10	1.28	1.24	1.23	1.48	1.48	1.21
M(3)	Al	0.11	0.14	0.25	0.14	0.21	0.21	0.17	0.27	0.28	0.27	0.11	0.27	0.32
	Mg	0.65	0.67	0.66	0.71	0.72	0.72	0.67	0.64	0.64	0.65	0.82	0.66	0.61
	*Fe ²⁺	0.24	0.19	0.09	0.15	0.07	0.07	0.16	0.09	0.08	0.08	0.07	0.07	0.07
M(4)	Mn ²⁺	0.01	0.01	0.01	0.01	0.01	0.01	0.01	0.01	0.01	0.01	0.01	0.01	0.01
	*Fe ²⁺	0.13	0.14	0.06	0.18	0.12	0.13	0.11	0.14	0.15	0.11	0.07	0.12	0.12
	Mg	0.02	0.04	-	0.04	0.03	0.02	0.03	0.04	0.05	0.08	0.01	0.07	0.07
	Ca	1.84	1.81	1.88	1.76	1.84	1.84	1.85	1.81	1.79	1.80	1.91	1.80	1.77
	Na	-	-	0.05	0.01	-	-	-	-	-	-	-	-	0.03

* Fe²⁺ includes minor Ni (< 0.014 apfu)

T(1) and T(2) sites

The Finero amphiboles are pargasitic, and contain significant [4]-coordinated Al (Table 6). The observed $\langle T(1)-O \rangle$ and $\langle T(2)-O \rangle$ distances indicate that the ^{14}Al is completely ordered at the $T(1)$ site, except perhaps for crystal F(1), in which the observed $\langle T(2)-O \rangle$ distance of 1.637 Å may indicate a small amount of ^{14}Al at the $T(2)$ site. The ^{14}Al estimates from EMPA are in good agreement with those obtained from the $\langle T(1)-O \rangle$ distances (Oberti *et al.* 1995a); note that the latter indicate a higher ^{14}Al content (0.10 apfu) for crystal F(4).

M(1) site

The site scattering and $\langle M(1)-O \rangle$ distances (Fig. 1b) indicate that $M(1)$ is occupied by Mg and Fe^{2+} . Site populations were therefore assigned directly from the refined site-scattering values. The $\langle M(1)-O \rangle$ distances calculated from these site populations are in good agreement with the observed distances, the difference (obs. - calc.) ranging from 0.001 to 0.003 Å.

M(2) site

The site scattering and $\langle M(2)-O \rangle$ distances indicate that $M(2)$ is occupied by Mg, Al, Fe^{2+} and Fe^{3+} ; in addition, electron-microprobe analysis shows minor amounts of Ti^{4+} and Cr^{3+} , which were assigned to $M(2)$, as there is no evidence of Ti^{4+} entering $M(1)$ via the oxy-substitution mechanism of Oberti *et al.* (1992). To derive the $M(2)$ site-populations, we solve a set of simultaneous linear equations involving the MAN, the $\langle M(2)-O \rangle$ distance, the constraint that the site be completely occupied, and the formal charge at that site. Normally, we calculate the mean formal charge (C) at the $M(2)$ site via the equation $2^{M(2)}C = {}^{\text{oct}}C - 2^{M(1)}C - {}^{M(3)}C = {}^{\text{oct}}C - 6.0$, where ${}^{\text{oct}}C$ is derived from the A -, B - and T -site populations with the constraint of overall neutrality of charges. For the Finero amphiboles, we cannot use this relationship, as the occurrence of Al at $M(3)$ means that the partitioning of ${}^{\text{oct}}C$ between $M(2)$ and $M(3)$ is unknown, and hence the set of linear equations cannot be solved.

We have argued above that the higher-valence transition-metals occur at the $M(2)$ site; these were so assigned. From the refined site-scattering values, the (Mg + Al) and Fe^{2+} populations were calculated. Following this, the Mg and Al contents were calculated from the $\langle M(2)-O \rangle$ versus $\langle {}^{M(2)}r \rangle$ equation of Hawthorne (1983).

M(3) site

The Al content of $M(3)$ was assigned via the equation ${}^{M(3)}\text{Al} = [{}^{16}\text{Al} - {}^{M(2)}\text{Al}]$ using the ^{16}Al content of the unit formula (Table 6). The Mg and Fe^{2+}

contents were then calculated directly from the refined scattering-values at $M(3)$ after allowing for the presence of Al at $M(3)$. The resulting site-populations are reported in Table 7.

$\langle M(3)-O \rangle$ AS A FUNCTION OF CONSTITUENT CATIONS

The $\langle M-O \rangle$ distances in amphiboles can be reasonably well represented as linear functions of the sizes of their constituent cations, either using ionic radii (Hawthorne 1978, 1983) or ideal mean bond-lengths (Ungaretti 1980, Cannillo *et al.* 1981). The Al content at $M(2)$ was assigned on the basis of mean bond-length, and hence $\langle M(2)-O \rangle$ must be linear with constituent cation radius according to the equation $\langle M(2)-O \rangle = 1.488 + 0.827 {}^{M(2)}\langle r \rangle$ of Hawthorne (1983). However, the Al content of $M(3)$ was assigned by difference, using the analytically determined ^{16}Al values and the ${}^{M(2)}\text{Al}$ values; hence the assignment of Al to $M(3)$ is independent of $\langle M(3)-O \rangle$. As we expect a linear relationship between $\langle M(3)-O \rangle$ and ${}^{M(3)}\langle r \rangle$, this will provide quite a stringent test of the $M(3)$ site-populations derived here. Figure 3 shows this relationship; the line represents the expected behavior on the basis of the relationship of Hawthorne (1983). A well-developed linear correlation occurs, showing that, despite the circuitous nature of the assignment process, the site-populations are consistent with the structural variations observed. Note that there is one outlier, crystal F(4). We noted above that this crystal shows poor agreement between the EMPA and SREF values, and that an increase of at least 0.10 ^{14}Al apfu is needed on the basis of the $\langle T(1)-O \rangle$ bond-length; obviously there is an error in the electron-microprobe analysis. If we subtract 0.10 ^{16}Al apfu from the $M(3)$ site-population of Table 7, we obtain 0.15 Al + 0.76 Mg + 0.09 Fe^{2+} , with ${}^{M(3)}\langle r \rangle$ of 0.697, in line with the expected trend. Of course, this shift implies some other

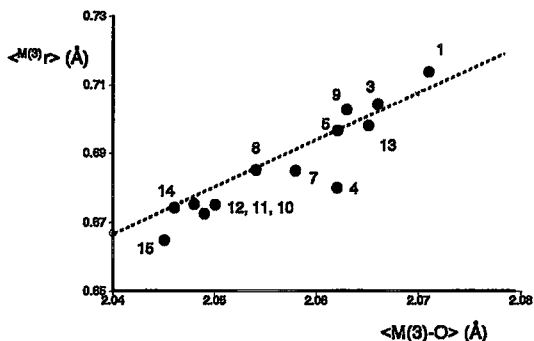


FIG. 3. Variation in $\langle M(3)-O \rangle$ as a function of mean radius of the constituent cations in the Finero suite of amphibole compositions; the line is the ideal relationship of Hawthorne (1983).

changes in order to maintain the overall charge-balance of the formula. We have included F(4) in this discussion to show that only *accurate* chemical and structural data can give fully consistent results, and that errors in the data do come to light, despite the complicated nature of the process of site-population assignment.

Hawthorne (1978, 1983) developed linear relationships between $\langle M-O \rangle$ bond-lengths and constituent cation (and anion) radii for the *M* sites in amphiboles. The relationship for the *M*(3) site is far less well-defined [$R = 0.925$] than the corresponding relationships for the *M*(1) [$R = 0.961$] and *M*(2) [$R = 0.997$] sites. It now seems probable that this nonlinearity for *M*(3) is due (at least in part) to the presence of an unrecognized trivalent-cation content at the *M*(3) site in previous structural studies of amphiboles. The presence of monovalent cations (Li, Na) at *M*(3) (Hawthorne *et al.* 1993) may also contribute to this nonlinearity.

DISORDER OF Al OVER THE OCTAHEDRAL SITES

The significant occupancy of *M*(3) by Al may be, in principle, related to the high temperature and pressure of crystallization and equilibration of the amphibole. In particular, the high temperature will have tended to promote disorder of cations over nonequivalent sites in the structure. However, Al is partly disordered over *M*(2) and *M*(3), but does not occur at *M*(1); hence there must be a strong crystal-chemical control preventing the occurrence of Al at *M*(1) while allowing Al to occur at *M*(3).

The relevant local charge-distributions in normal (ideal) pargasite and pargasite containing Al at *M*(1)

and *M*(3) are shown in Table 8 using bond-strength tables. There are two (most probable) arrangements of local charge in normal pargasite (Tables 8a, b). Where *M*(2) is occupied by Mg, *T*(1) is locally occupied by Si, leading to the bond-strength sums shown in Table 8a and an arrangement of charges characteristic of tremolite. Where *M*(2) is occupied by Al, *T*(1) is locally occupied by Al, leading to reasonable bond-strength sums around O(1), O(2) and O(3). An exchange of Al and Mg between *M*(2) and *M*(1) or between *M*(2) and *M*(3) will modify the charge arrangement from b to c and d, respectively (Table 8). The results of both these exchanges indicate a large bond-strength excess on O(3) (1.33 and 1.17 v.u., respectively), which can be alleviated only by relaxing *M*(1)-O(3) and *M*(3)-O(3); this explains why Al is normally ordered at the *M*(2) site in amphiboles where $O(3) = (OH,F,Cl)_2$. If some $[6]R^{3+}$ disorder has to occur for any reason, the very high bond-strength excess at O(3) that would result from this arrangement prevents the occurrence of Al at *M*(1).

COMPARISON WITH RESULTS ON SYNTHESIS AMPHIBOLE

Raudsepp *et al.* (1987, 1991) reported the hydrothermal synthesis of pargasite of nominal composition $NaCa_2[Mg_4M^{3+}]Si_6Al_2O_{22}W_2$, where $M^{3+} = Al, Co^{3+}, Sc, In$, and $W = OH, F$. In the hydroxyl series, they examined the synthesized amphiboles by infrared spectroscopy in the principal OH-stretching region, and showed that the trivalent cations are disordered over the [*M*(1) + *M*(3)] and *M*(2) sites. Welch *et al.* (1994) obtained identical results for synthetic pargasite by infrared (IR) spectroscopy. Their 2H MAS NMR

TABLE 8. LOCAL CHARGE ARRANGEMENTS AND BOND-STRENGTH TABLES FOR POSSIBLE ARRANGEMENTS OF [6]-COORDINATED Al IN PARGASITE

(a) Pargasite with Mg at M(2)								(b) Pargasite with Al at M(2)							
	M(1)	M(2)	M(3)	M(4)	T(1)	T(2)	Σ		M(1)	M(2)	M(3)	M(4)	T(1)	T(2)	Σ
O(1)	1/3	1/3	1/3		1.0		2.00	O(1)	1/3	1/2	1/3		3/4		1.92
O(2)	1/3	1/3		1/4		1.0	1.92	O(2)	1/3	1/2		1/4		1.0	2.08
O(3)	1/3 ^{al} →		1/3				1.00	O(3)	1/3 ^{al} →		1/3				1.00
(c) Pargasite with Al at M(1)								(d) Pargasite with Al at M(3)							
	M(1)	M(2)	M(3)	M(4)	T(1)	T(2)	Σ		M(1)	M(2)	M(3)	M(4)	T(1)	T(2)	Σ
O(1)	1/2	1/3	1/3		3/4		1.92	O(1)	1/3	1/2	1/2		3/4		1.92
O(2)	1/2	1/3		1/4		1.0	2.08	O(2)	1/3	1/3		1/4		1.0	1.92
O(3)	1/2 ^{al} →		1/3				1.33	O(3)	1/3 ^{al} →		1/2				1.17

spectrum also shows that Al occurs at $M(1) + M(3)$ [not $M(3)$ as stated], and comparison of the ^{27}Al MAS NMR with and without cross-polarization indicates that ^{61}Al occurs at $M(2)$ as well as $M(1) + M(3)$. In the fluorine series, Raudsepp *et al.* (1987) showed by Rietveld structure refinement that Sc and In are ordered at the $M(2)$ site; Al ordering at $M(2)$ has been recently shown by SREF studies of synthetic F-pargasite (Oberti *et al.* 1995b). The infrared results of Raudsepp *et al.* (1987) for the hydroxyl pargasite series could not distinguish between trivalent cations at the $M(1)$ and $M(3)$ sites. However, they also determined the site populations of scandium-pargasite by Rietveld structure refinement, showing that the $M(1)$ site is fully occupied by Mg, and that Sc occurs at $M(2)$ and $M(3)$; this is *exactly* in line with the occurrence of Al at $M(2)$ and $M(3)$ in the Finero amphiboles examined here. The disorder in the hydroxyl pargasite series observed by Raudsepp *et al.* (1987) seemed at that time to be at odds with the generally accepted model (Hawthorne 1983) that [6]-coordinated trivalent cations are invariably ordered at the $M(2)$ site in (unoxidized) amphiboles. Raudsepp *et al.* (1987) tried to induce changes in ^{61}Al order (as reflected in the OH-stretching spectrum) by annealing synthetic pargasite at a variety of temperatures and times, but no changes were observed. It is apparent from the results obtained here that natural pargasite and pargasitic hornblende (at least those crystallized at high pressures and temperatures) have considerable ^{61}Al disorder over the $M(2)$ and $M(3)$ sites, and the results of Raudsepp *et al.* (1987, 1991) and Welch *et al.* (1994) do seem to represent the equilibrium state of pargasite.

^{61}Al DISORDER:

AN EFFECT OF COMPOSITION OR CONDITIONS OF CRYSTALLIZATION?

The Finero amphiboles have two distinct characteristics in addition to ^{61}Al disorder: (1) they are generally very Fe-poor, and (2) they crystallized at relatively high temperatures and high pressures. Of course, these two features are not totally independent. In order to crystallize at such conditions, the amphibole must be Fe-poor, as Fe-rich pargasite is not stable under such conditions. However, which is the dominant factor that causes the disorder, the composition or the conditions of crystallization? Pertinent to this problem are the results of Raudsepp *et al.* (1987). They synthesized Fe-free pargasite at 700°C and 1 kbar, conditions far below those extant during the crystallization of the Finero amphiboles, and showed by IR spectroscopy that the synthesized pargasite has ^{61}Al disorder over $M(1) + M(3)$. This observation indicates that it is the composition of the amphibole, rather than the conditions of crystallization, that seems to be the primary factor involved in ^{61}Al disorder. The fact that pargasite from other localities shows the same (even if

less extreme) pattern of $\langle M(1)-O \rangle$ and $\langle M(3)-O \rangle$ distances (see Fig. 2, lined area) is concordant with this conclusion.

Pargasite (with 2 $^{41}\text{R}^{3+}$ and 1 $^{61}\text{R}^{3+}$ apfu) is probably the only amphibole end-member in which local charge-balance constraints allow some $^{61}\text{R}^{3+}$ disorder between the $M(2)$ and $M(3)$ sites. The bond-strength deficiencies at the anions coordinating Al at $T(1)$ are balanced, in the case of O(5), O(6) and O(7), by the maximum possible bond-strength contributions from the A and $M(4)$ cations. The bond-strength requirement of the apical O(1) has to be satisfied by relaxation within the strip of octahedra, particularly around the $M(1)$ and $M(3)$ sites. However, $M(3)$ is much more effective than $M(1)$ in this regard, as the $M(3)$ cation coordinates four O(1) atoms. Moreover, $^{61}\text{R}^{3+}$ at $M(1)$ results in a much larger excess of incident bond-strength at O(3) than does $^{61}\text{R}^{3+}$ at $M(3)$ (Table 8). These two factors indicate that $^{61}\text{R}^{3+}$ substitution at $M(3)$ is the best crystal-chemical solution to this problem. Furthermore, the presence of some $^{61}\text{R}^{3+}$ at $M(3)$ helps to alleviate the overbonding on O(2) that is present if all $^{61}\text{R}^{3+}$ is ordered at $M(2)$.

It is notable that synthetic fluor-pargasite behaves differently from pargasite in that the former has $^{61}\text{R}^{3+}$ completely ordered at the $M(2)$ site (Oberti *et al.* 1995b). In order to account for the effect of F on $^{61}\text{R}^{3+}$ ordering, we note that F substitution at O(3) shortens the $M(1)-O(3)$ and $M(3)-O(3)$ distances, in contrast with the relaxations associated with the local charge-arrangement discussed above; this effect will be discussed in more detail in a later manuscript on ordering in amphiboles.

Disorder involving $^{61}\text{R}^{3+}$ is lower in Fe-rich pargasite (see Fig. 1a). The enlargement of the $M(3)$ site due to $\text{Fe} \rightarrow \text{Mg}$ substitution is obviously in contrast to the contractions associated with the occurrence of smaller $^{61}\text{R}^{3+}$ cations at $M(3)$, and probably allows more structural relaxation around O(3).

SOLID SOLUTION OF AN (Fe-Mg-Mn)-AMPHIBOLE COMPONENT IN FINERO PARGASITE

Both the electron-microprobe results (Table 6) and the SREF results (Table 4) indicate significant (Mn,Fe,Mg) at the $M(4)$ site; this occupancy of $M(4)$ may be regarded as solid solution of a ferromagnesian amphibole component in the structure of a calcic amphibole. The magnitude of this component, as derived from the renormalization of the electron-microprobe results, is very sensitive to the following factors: (1) errors in the analysis itself, (2) use of an incorrect Fe^{3+} content, and (3) use of an inappropriate scheme for renormalization. Thus it is pertinent to question whether the (Mn,Fe,Mg) site-populations for $M(4)$ are reliable, particularly as they vary in the range 0.07–0.23 apfu (Table 7) in the amphiboles characterized in this work.

Agreement between SREF and EMP data

The effective scattering at the *M*(4) site, as calculated from the electron-microprobe results and as measured by site-scattering refinement, has a mean discrepancy of 0.2 *e*. This corresponds to a difference in Ca-Fe occupancy of 0.03 apfu, indicating that the range of values noted above (0.07–0.23 apfu) is significant. However, the site-scattering refinement results cannot be considered to fully confirm the electron-microprobe results and the resultant site-populations, as we have assigned five distinct cations to the *M*(4) site, but we used only the constraints of observed site-scattering, full occupancy, and overall neutrality. Thus, although the two sets of values are fully compatible, we would like additional confirmation in terms of the physical-chemical reasonableness of the site populations.

Variation in (Fe,Mg,Mn) at M(4)

In Table 9, the amphiboles are listed according to their paragenesis, together with their ^{*M*(4)}(Fe + Mg + Mn) contents. It is immediately apparent that the significant variations in ^{*M*(4)}(Fe + Mg + Mn) content are paragenetically related. Within specific units, the values are very similar. Of course, there are differences where the associated assemblages are very different, as in the case of F(3) and F(5), which both occur in the LIZ (Layered Internal Zone) in the southeastern part of the intrusion, but in very different assemblages (see Table 1). However, the correlation of the (Fe + Mg + Mn) content of *M*(4) with petrological environment strongly suggests that our combined use of SREF and EMP gives accurate results.

Single-phase ferromagnesian amphiboles invariably show the *M*(4) site-preference Mn > Fe > Mg.

Inspection of Table 7 shows that this is also the case for the calcic amphiboles of this work; similar results have been obtained by Oberti *et al.* (1993) in the case of manganoan richterite. Ghose & Weidner (1972) have shown that ordering of Fe²⁺ and Mg between *M*(4) and *M*(1,2,3) in ferromagnesian amphiboles is a function of composition and cooling history. Are there any systematics in the Finero data? Also listed in Table 9 are the Mg/(Fe + Mg + Mn) values at the *M*(4) site of the amphiboles characterized here. Inspection of Table 9 shows a considerable measure of coherence in these values for specific parageneses, lending further credence to the validity of these results.

CONCLUSIONS

1. ⁶Al is partly disordered over the *M*(2) and *M*(3) sites in pargasite and pargasitic hornblende from the Finero mafic-ultramafic complex.
2. This type of occupancy has not been recognized previously, and accounts for a major part of the scatter associated with previously developed relationships between <*M*(3)-O> and constituent site-composition or mean cation-radius.
3. This disorder is in accord with previous spectroscopic and Rietveld structure work on synthetic pargasite, which also shows disorder of trivalent cations over the octahedral sites in the (hydroxy) amphibole structure.
4. ⁶Al does not occur at *M*(1) in these amphiboles; this can be explained on the basis of the high bond-strength excess at the O(3) site if ⁶R³⁺ enters the *M*(1) site. This substitution can occur only in the presence of dehydrogenation, which lowers this excess.
5. The occurrence of ⁶Al and Sc³⁺ at *M*(3) in synthetic amphiboles synthesized at low temperatures and pressures indicates that the occurrence of ⁶Al at *M*(3) in the amphiboles from Finero is not a direct result of their high temperatures and pressures of crystallization. The occurrence of this ⁶R³⁺ disorder is related to the particularly Fe-poor compositions. Moreover, ⁶R³⁺ disorder is inhibited by the occurrence of F at O(3).
6. The Finero amphiboles have considerable (up to 11.5%) solid solution of ferromagnesian amphibole component in their structure; the amount of ferromagnesian amphibole component correlates very strongly with paragenesis.

ACKNOWLEDGEMENTS

We are very grateful to Franca Siena and Massimo Coltorti for supplying such well-documented material for study. FCH was supported by a Killam Fellowship and an Operating Grant from the Natural Sciences and Engineering Research Council of Canada. We are grateful for the comments of the referees and the Associate Editor, which contributed to the clarity of the paper.

TABLE 9. DETAILS OF FERROMAGNESIAN AMPHIBOLE SOLID-SOLUTION IN THE CALCIC AMPHIBOLES FROM THE FINERO COMPLEX

Rock unit	^{<i>M</i>(4)} (Fe+Mg+Mn)	^{<i>M</i>(4)} [Mg/(Fe+Mg+Mn)]
F(13) Phlogopite peridotite	0.09	0.11
F(1) Amphibole peridotite	0.16	0.12
F(7) Amphibole peridotite	0.16	0.19
F(8) Amphibole peridotite	0.16	0.12
F(9) Amphibole peridotite	0.15	0.20
F(3) LIZ (SE) - peridotite	0.19	0.21
F(10) LIZ (NW) - olivine websterite	0.19	0.21
F(11) LIZ (NW) - sapphirine gabbro	0.21	0.24
F(12) LIZ (NW) - sapphirine gabbro	0.20	0.38
F(14) LIZ (NW) - sapphirine gabbro	0.20	0.35
F(15) LIZ (NW) - sapphirine gabbro	0.20	0.35
F(5) LIZ (SE) - gabbro	0.23	0.17

Note: F(4) has been omitted because of the low reliability of the chemical analysis (see text).

REFERENCES

- CANNILLO, E., OBERTI, R. & UNGARETTI, L. (1981): CORANF, un programma per il calcolo e la elaborazione di parametri chimici e geometrici degli anfibioli. *Rend. Soc. Ital. Mineral. Petrol.* **37**, 613-621.
- CAWTHORN, R.G. (1975): The amphibole peridotite—metagabbro complex, Finero, northern Italy. *J. Geol.* **83**, 437-454.
- _____ & O'HARA, M.J. (1976): Amphibole fractionation in calc-alkaline magma genesis. *Am. J. Sci.* **276**, 309-329.
- COLTORTI, M. & SIENA, F. (1984): Mantle tectonite and fractionate peridotite at Finero (Italian Western Alps). *Neues Jahrb. Mineral. Abh.* **149**, 225-244.
- GHOSE, S. & WEIDNER, J.R. (1972): Mg²⁺–Fe²⁺ order–disorder in cumingtonite, (Mg,Fe)₇Si₈O₂₂(OH)₂: a new geothermometer. *Earth Planet. Sci. Lett.* **16**, 346-354.
- HAWTHORNE, F.C. (1978): The crystal chemistry of the amphiboles. VI. The stereochemistry of the octahedral strip. *Can. Mineral.* **16**, 37-52.
- _____ (1983): The crystal chemistry of the amphiboles. *Can. Mineral.* **21**, 173-480.
- _____, UNGARETTI, L., OBERTI, R. & BOTTAZZI, P. (1993): Li: an important component in igneous alkali amphiboles. *Am. Mineral.* **78**, 733-745.
- LENSCH, G. (1968): Die Ultramafitite der Zone von Ivrea und ihre geologische Interpretation. *Schweiz. Mineral. Petrogr. Mitt.* **48**, 91-102.
- _____ (1976): Ariegite und Websterite in Lherzolite von Balmuccia (Val Sesia/Zone von Ivrea). *Neues Jahrb. Mineral. Abh.* **128**, 189-208.
- OBERTI, R., CANNILLO, E., UNGARETTI, L. & HAWTHORNE, F.C. (1995a): Temperature-dependent Al order–disorder in the tetrahedral double-chain of C2/m amphiboles. *Eur. J. Mineral.* (in press).
- _____, HAWTHORNE, F.C., UNGARETTI, L. & CANNILLO, E. (1993): The behaviour of Mn in amphiboles: Mn in richterite. *Eur. J. Mineral.* **5**, 43-51.
- _____, SARDONE, N., HAWTHORNE, F.C., RAUDSEPP, M. & TURNOCK, A.C. (1995b): Synthesis and crystal-structure refinement of synthetic fluor-pargasite. *Can. Mineral.* **33**, 25-31.
- _____, UNGARETTI, L., CANNILLO, E. & HAWTHORNE, F.C. (1992): The behaviour of Ti in amphiboles. I. Four- and six-coordinated Ti in richterites. *Eur. J. Mineral.* **4**, 425-439.
- OTTONELLO, G., ERNST, W.G. & JORON, J.L. (1984): Rare earth and 3rd transition element geochemistry of peridotitic rocks. I. Peridotites from the Western Alps. *J. Petrol.* **25**, 343-372.
- RAUDSEPP, M., TURNOCK, A.C. & HAWTHORNE, F.C. (1991): Amphibole synthesis at low pressure: what grows and what doesn't. *Eur. J. Mineral.* **3**, 983-1004.
- _____, _____, _____, SHERRIFF, B.L. & HARTMAN, J.S. (1987): Characterization of synthetic pargasitic amphiboles (NaCa₂Mg₄M³⁺Si₆Al₂O₂₂(OH,F)₂; M³⁺ = Al, Cr, Ga, Sc, In) by infrared spectroscopy, Rietveld structure refinement, and ²⁷Al, ²⁹Si and ¹⁹F MAS NMR spectroscopy. *Am. Mineral.* **72**, 580-593.
- RIVALENTI, G., GARUTI, G. & ROSSI, A. (1975): The origin of the Ivrea–Verbano basic formation (Italian Western Alps) – whole rock geochemistry. *Boll. Soc. Geol. Ital.* **94**, 1149-1186.
- _____, _____, _____, SIENA, F. & SINIGOI, S. (1981): Existence of different peridotite types and of a layered igneous complex in the Ivrea Zone of the Western Alps, Italy. *J. Petrol.* **22**, 127-153.
- _____, ROSSI, A., SIENA, F. & SINIGOI, S. (1984): The layered series of the Ivrea–Verbano igneous complex, Western Alps, Italy. *Tschermaks Mineral. Petrogr. Mitt.* **33**, 77-99.
- SIENA, F. & COLTORTI, M. (1989): The petrogenesis of a hydrated mafic–ultramafic complex and the role of amphibole fractionation at Finero (Italian Western Alps). *Neues Jahrb. Mineral. Monatsh.*, 255-274.
- UNGARETTI, L. (1980): Recent developments in X-ray single crystal diffractometry applied to the crystal-chemical study of amphiboles. *God. Jug. Cen. Kristalogr.* **15**, 29-65.
- _____, MAZZI, F., ROSSI, G. & DAL NEGRO, A. (1981): Crystal-chemical characterization of blue amphiboles. In *Proc. Eleventh Gen. Meet., Int. Mineral. Assoc., Rock-Forming Minerals* (A.V. Sidorenko, ed.), Nauka, Moscow (82-110).
- WELCH, M.D., KOLODZIEJSKI, W. & KLINOWSKI, J. (1994): A multinuclear NMR study of synthetic pargasite. *Am. Mineral.* **79**, 261-268.

Received April 28, 1994, revised manuscript accepted September 13, 1994.